



# CONTROL OF A TWO-LINK RIGID-FLEXIBLE MANIPULATOR WITH A MOVING PAYLOAD MASS

S. CHOURA

*Departement de Préparation Au Concours Technologique, Institut Préparatoire Aux Etudes  
d'Ingénieurs de Sfax B.P. 805 Sfax 3018, Tunisia*

AND

A. S. YIGIT

*Department of Mechanical and Industrial Engineering Kuwait University, P.O. Box 5969, Safat 13060,  
Kuwait*

*(Received 16 May 2000, and in final form 11 September 2000)*

Control of a two-link rigid-flexible manipulator carrying a moving payload mass is considered. The stability of the system when the payload mass is moving along the flexible link during the time of maneuver is investigated. A candidate Lyapunov function is constructed and its time rate of change is examined. It is shown that the use of an independent PD-type controller yields a convergence of residual vibration to zero, an attainment of the rigid-body rotations to their prespecified desired angles of maneuver, and an axial guidance of the payload mass. It is shown that allowing the relative motion of the payload mass, as it moves along the flexible link, leads to a considerable reduction of its residual vibrations as compared with the case when it is fixed to the link tip during the time of maneuver. The performance of the proposed controller is also verified in case the links and the payload mass are required to track prespecified reference trajectories.

© 2001 Academic Press

## 1. INTRODUCTION

In industry, certain robot manipulations consist of moving objects from one location to another with high accuracy. It is known that high-speed maneuvers are often required for raising line production. However, large rotational speeds induce flexural vibration of lightweight links due to inertial effects; and thus, the positional accuracy may not be guaranteed in the presence of vibrations. To overcome this, stabilizing controllers are typically applied at the joints for two reasons: to position the links to their desired locations, and to reduce the residual vibration at and after the maneuver time [1, 2].

There has been extensive research on control of flexible manipulators, (see e.g., references [3–5]). Most of the control strategies proposed in the literature are model based. In other words, the controller gains are obtained based on a model and its nominal parameters. The main drawback of all model-based controllers is that one never has an exact model. Therefore, the robustness to parameter uncertainties has been a major concern in control design for manipulators, which leads to various robust-control applications [6–8]. Another difficulty with the flexible systems is the so-called “spillover” problem. Since the actual system is a distributed parameter system, any controller design based on finite dimensional models will generally suffer from the control and observation spillovers: The control action will also affect the neglected higher modes, and the measurements will also contain the effect

of higher modes [9]. To address both robustness and spillover problem, non-model based controllers which are derived by using Lyapunov techniques have been developed [10–12]. Yigit [2] has employed proper Lyapunov functions to conclude that independent PD joint controllers stabilize the overall dynamics of a two-link rigid–flexible manipulator. These functions do not require any discretization of the distributed system, and yield a control law which does not suffer from any control or observation spillover. The control law is generally chosen to make the rate of change of a candidate Lyapunov function negative. Experimental work verifying the efficacy of joint controllers has appeared in references [13, 14].

In common practice, robot manipulators retain the object or payload mass fixed at the tip of the end-link during maneuver. Therefore, controllers are designed based on a fixed payload mass. Clearly, not all applications require a fixed payload. Thus some valid questions can be posed: (1) If the payload mass is guaranteed to be at the tip of the end-link at the end of the maneuver time, can it be allowed to move during maneuver along the link in a prescribed manner? (2) Can this motion be utilized to reduce the residual vibration in the link more rapidly? To the best of the authors' knowledge, current commercial robotic manipulators do not have relative motion of payload mass with respect to the end link. However, some modern machining systems have loading systems with moving payload mass. It is also common to see moving payload mass in cranes. Clearly, this additional motion allows the use of more complex trajectories and increases the speed of maneuver. The results of the current study shows that the relative payload motion can improve the dynamic behavior significantly, and allow faster maneuver.

Though the beneficial effect of a moving payload was shown on a single-link arm in reference [15], as is well known, a single-link case does not have sufficient kinematic complexity to generalize the results for practical multi-link manipulators. The kinematic non-linearities introduced by the additional link, as well as dynamic non-linearities such as centrifugal and coriolis effects due to the moving payload mass complicates the dynamic behavior. Thus, the objective of the current study is to investigate the effects of payload relative motion in a two-link rigid–flexible manipulator, and to design efficient controllers which exploit this effect.

The remainder of this paper is organized as follows. Section 2 is devoted to mathematical modelling for the two-link rigid–flexible manipulator. Section 3 studies the stability of the resulting dynamics under the effect PD type controllers. Section 4 contains the simulation results and discussion of the effect of the payload dynamics on the residual vibration of the flexible link. In section 5 the controller is generalized for tracking reference trajectories, and contains simulation results showing the performance of proposed controller. Finally, summary and conclusions are given in section 6.

## 2. DYNAMIC MODELLING

Consider the horizontal-planar motion of a two-link rigid–flexible manipulator shown in Figure 1, where the rigid link is assumed to be uniform. The flexible link is clamped to the rigid base and is assumed to be thin and uniform, and satisfies the Euler–Bernoulli beam assumptions of small shear and rotary inertia effects. The payload mass is allowed to move without friction relative to the flexible link with a force actuator. Depending on the amount of flexibility and the power requirement, different actuators can be employed for this purpose. For example, for heavy duty applications a ball screw arrangement may be suitable whereas for lightweight payloads and more flexible links a transmission belt or cable system along with guide rails may be more feasible. In addition to the force actuator, two torque actuators are placed at the rigid bases for controlling the rotations of the links.

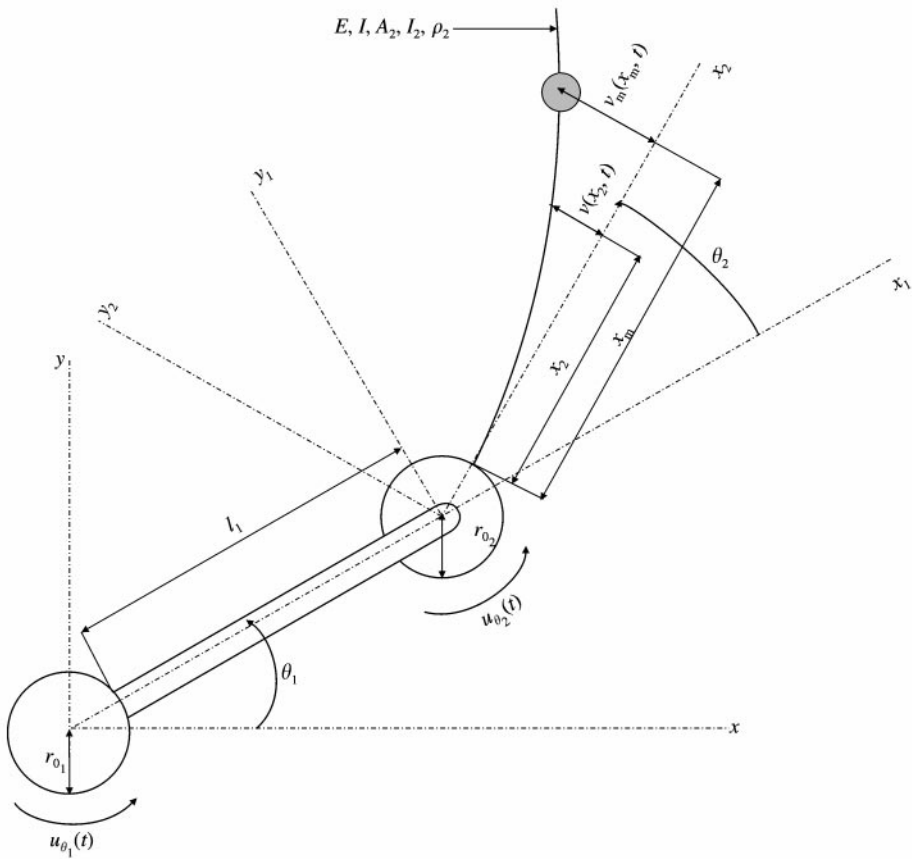


Figure 1. Two-link rigid—flexible manipulator.

Consider two frames of reference: the  $x_1 - y_1$  and  $x_2 - y_2$  frames are fixed to the rigid bases with angular velocities  $\dot{\theta}_1$  and  $\dot{\theta}_1 + \dot{\theta}_2$ , respectively. The unit vectors associated with these frames satisfy

$$\mathbf{i}_2 = \cos \theta_2 \mathbf{i}_1 + \sin \theta_2 \mathbf{j}_1, \quad \mathbf{j}_2 = -\sin \theta_2 \mathbf{i}_1 + \cos \theta_2 \mathbf{j}_1. \tag{1}$$

The position vectors locating an infinitesimal mass element on the rigid and flexible links; the second rigid base and the moving payload mass are given by

$$\mathbf{r}_1(x_1, t) = (r_{01} + x_1)\mathbf{i}_1, \quad \mathbf{r}_{h_2} = (r_{01} + l_1)\mathbf{i}_1,$$

$$\mathbf{r}_2(x_2, t) = [(r_{01} + l_1) + (r_{02} + x_2) \cos \theta_2 - v \sin \theta_2]\mathbf{i}_1 + [(r_{02} + x_2) \sin \theta_2 + v \cos \theta_2]\mathbf{j}_1,$$

$$\mathbf{r}_m(x_m, t) = [r_{01} + l_1 + (r_{02} + x_m) \cos \theta_2 - v_m \sin \theta_2]\mathbf{i}_1 + [(r_{02} + x_m) \sin \theta_2 + v_m \cos \theta_2]\mathbf{j}_1, \tag{2}$$

where  $v = v(x_2, t)$  and  $v_m = v(x_m, t)$ . The time derivatives of the unit vectors  $\mathbf{i}_1$  and  $\mathbf{j}_1$  are given by  $d\mathbf{i}_1/dt = \dot{\theta}_1\mathbf{j}_1$  and  $d\mathbf{j}_1/dt = -\dot{\theta}_1\mathbf{i}_1$ . It can be shown that the velocity vectors

reduce to

$$\begin{aligned}
 \dot{\mathbf{r}}_1 &= (r_{0_1} + x_1)\dot{\theta}_1 \mathbf{j}_1, & \dot{\mathbf{r}}_{h_2} &= (r_{0_1} + l_1)\dot{\theta}_1 \mathbf{j}_1, \\
 \dot{\mathbf{r}}_2 &= -[(r_{0_2} + x_2)\dot{\theta} \sin \theta_2 + v \dot{\theta} \cos \theta_2 + \dot{v} \sin \theta_2] \mathbf{i}_1 \\
 &\quad + [(r_{0_1} + l_1)\dot{\theta}_1 + (r_{0_2} + x_2)\dot{\theta} \cos \theta_2 - v \dot{\theta} \sin \theta_2 + \dot{v} \cos \theta_2] \mathbf{j}_1, \\
 \dot{\mathbf{r}}_m &= [\dot{x}_m \cos \theta_2 - (r_{0_2} + x_m)\dot{\theta} \sin \theta_2 - v_m \dot{\theta} \cos \theta_2 - \dot{v}_m \sin \theta_2 - \dot{x}_m v'_m \sin \theta_2] \mathbf{i}_1 \\
 &\quad + [(r_{0_1} + l_1)\dot{\theta}_1 + (r_{0_2} + x_m)\dot{\theta} \cos \theta_2 - v_m \dot{\theta} \sin \theta_2 + \dot{x}_m \sin \theta_2 \\
 &\quad + \dot{v}_m \cos \theta_2 + \dot{x}_m v'_m \cos \theta_2] \mathbf{j}_1,
 \end{aligned} \tag{3}$$

where the dot and prime signs associated with  $v_m$  denote  $\partial/\partial t$  and  $\partial/\partial x_m$ , respectively, and

$$\theta = \theta_1 + \theta_2.$$

The total kinetic energy of the two-link manipulator can be written as

$$\begin{aligned}
 T &= \frac{1}{2} I_{h_1} \dot{\theta}_1^2 + \frac{1}{2} I_{h_2} \dot{\theta}^2 + \frac{1}{2} m_{h_2} \dot{\theta}_1^2 (r_{0_1} + l_1)^2 + \frac{1}{2} \rho_1 A_1 \dot{\theta}_1^2 \int_0^{l_1} (r_{0_1} + x_1)^2 dx_1 \\
 &\quad + \frac{1}{2} \rho_2 A_2 \int_0^{l_2} \dot{r}_2 \cdot \dot{r}_2 dx_2 + \frac{1}{2} m \dot{r}_m \cdot \dot{r}_m,
 \end{aligned} \tag{4}$$

where  $\rho_1$  and  $\rho_2$  are the densities of the link materials respectively.  $A_1$  and  $A_2$  are cross-sectional areas of the rigid link and flexible link, respectively,  $I_{h_1}$  and  $I_{h_2}$  are the mass moments of inertia of the rigid bases respectively. The strain energy resulting from the link flexural vibration is given by

$$U = \frac{1}{2} \int_0^{l_2} EI(v'')^2 dx_2, \tag{5}$$

where  $EI$  is the beam flexural rigidity and the prime sign associated with  $v$  denotes  $\partial/\partial x_2$ . The extended Hamilton's principle can be applied for deriving the equations of motion,

$$\int_{t_1}^{t_2} \delta(T - U) dt + \int_{t_1}^{t_2} \delta W dt = 0, \tag{6}$$

where the virtual work done by the external forces is given by

$$\delta W = u_{\theta_1} \delta\theta_1 + u_{\theta_2} \delta\theta_2 + u_{x_m} \delta x_m, \tag{7}$$

where  $u_{\theta_1}$ , and  $u_{\theta_2}$  are the joint torques and  $u_{x_m}$  is the control force applied to the payload. Substituting equations (4), (5) and (7) into equation (6), integrating by parts, and simplifying the resulting equation lead to the following non-linear coupled equations of motion and the

associated boundary conditions:

$$\begin{aligned}
 u_{\theta_1} = & I_{T_1} \ddot{\theta}_1 + I_T \ddot{\theta} + \rho_2 A_2 \int_0^{l_2} [2v\dot{\theta} + v^2\ddot{\theta} + (r_{0_2} + x_2)\ddot{v}] \\
 & - (r_{0_1} + l_1) \sin \theta_2 (2\ddot{\theta}_1 v + \ddot{\theta}_2 v + 2\dot{\theta} \dot{v}) - (r_{0_1} + l_1) \cos \theta_2 (\dot{\theta}_2^2 v + 2\dot{\theta}_1 \dot{\theta}_2 v - \ddot{v}) dx_2 \\
 & + \frac{1}{2} \rho_2 A_2 (r_{0_1} + l_1) [(r_{0_2} + l_2)^2 - r_{0_2}^2] [(2\ddot{\theta}_1 + \ddot{\theta}_2) \cos \theta_2 - (\dot{\theta}_2^2 + 2\dot{\theta}_1 \dot{\theta}_2) \sin \theta_2] \\
 & + m [(r_{0_2} + x_m) ((r_{0_2} + x_m) \ddot{\theta} + 2\dot{x}_m \dot{\theta} + \ddot{x}_m v'_m + 2\dot{x}_m v'_m + \dot{x}_m^2 v''_m + \ddot{v}_m) \\
 & + 2v_m \dot{v}_m \dot{\theta} + 2v_m v'_m \dot{x}_m \dot{\theta} + v_m^2 \ddot{\theta} - \ddot{x}_m v_m] \\
 & + m (r_{0_1} + l_1) \cos \theta_2 [(r_{0_2} + x_m) (2\ddot{\theta}_1 + \ddot{\theta}_2) + 2\dot{\theta} \dot{x}_m - \dot{\theta}_2^2 v_m - 2\dot{\theta}_1 \dot{\theta}_2 v_m \\
 & + \ddot{v}_m + 2\dot{v}'_m \dot{x}_m + \ddot{x}_m v'_m + \dot{x}_m^2 v''_m] \\
 & - m (r_{0_1} + l_1) \sin \theta_2 [(r_{0_2} + x_m) (2\dot{\theta}_1 \dot{\theta}_2 + \dot{\theta}_2^2) \\
 & + (2\ddot{\theta}_1 + \ddot{\theta}_2) v_m + 2\dot{\theta} \dot{v}_m + 2\dot{\theta} \dot{x}_m v'_m - \ddot{x}_m], \tag{8}
 \end{aligned}$$

$$\begin{aligned}
 u_{\theta_2} = & I_{T_2} \ddot{\theta}_2 + I_T \ddot{\theta} + \rho_2 A_2 \int_0^{l_2} [2v\dot{\theta} + v^2\ddot{\theta} + (r_{0_2} + x_2)\ddot{v}] \\
 & - \dot{\theta}_1 v (r_{0_1} + l_1) \sin \theta_2 + \dot{\theta}_1^2 v (r_{0_1} + l_1) \cos \theta_2 dx_2 \\
 & + \frac{1}{2} \rho_2 A_2 [(r_{0_2} + l_2)^2 - r_{0_2}^2] (r_{0_1} + l_1) (\ddot{\theta}_1 \cos \theta_2 + \dot{\theta}_1^2 \sin \theta_2) \\
 & + m [(r_{0_2} + x_m) ((r_{0_2} + x_m) \ddot{\theta} + 2\dot{x}_m \dot{\theta} + \ddot{x}_m v'_m + 2\dot{x}_m v'_m + \dot{x}_m^2 v''_m + \ddot{v}_m) \\
 & + 2v_m \dot{v}_m \dot{\theta} + 2v_m v'_m \dot{x}_m \dot{\theta} + v_m^2 \ddot{\theta} - \ddot{x}_m v_m] \\
 & + m (r_{0_1} + l_1) [(r_{0_2} + x_m) (\ddot{\theta}_1 \cos \theta_2 + \dot{\theta}_1^2 \sin \theta_2) + \dot{\theta}_1^2 v_m \cos \theta_2 - \ddot{\theta}_1 v_m \sin \theta_2], \tag{9}
 \end{aligned}$$

$$\begin{aligned}
 u_{x_m} = & m [\ddot{x}_m + \ddot{x}_m (v'_m)^2 + 2\dot{x}_m v'_m \dot{v}'_m + \dot{x}_m^2 v'_m v''_m \\
 & + \ddot{\theta} v'_m (r_{0_2} + x_m) + \ddot{v}_m v'_m - \ddot{\theta} v_m - 2\dot{\theta} \dot{v}_m - v_m v'_m \dot{\theta}^2 - (r_{0_2} + x_m) \dot{\theta}^2 \\
 & + (r_{0_1} + l_1) (\ddot{\theta}_1 \sin \theta_2 + \ddot{\theta}_1 v'_m \cos \theta_2 - \dot{\theta}_1^2 \cos \theta_2 + \dot{\theta}_1^2 v'_m \sin \theta_2)], \tag{10}
 \end{aligned}$$

$$\begin{aligned}
 0 = & E I v'''' + \rho_2 A_2 [\ddot{v} + (r_{0_2} + x_2) \ddot{\theta} + \ddot{\theta}_1 (r_{0_1} + l_1) \cos \theta_2 + \dot{\theta}_1^2 (r_{0_1} + l_1) \sin \theta_2 - v \dot{\theta}^2] \\
 & + m [-v_m \dot{\theta}^2 + 2\dot{x}_m \dot{\theta} + (r_{0_1} + l_1) \dot{\theta}_1^2 \sin \theta_2 + \ddot{v}_m + 2\dot{x}_m \dot{v}'_m + \ddot{x}_m v'_m + \dot{x}_m^2 v''_m \\
 & + (r_{0_2} + x_m) \ddot{\theta} + (r_{0_1} + l_1) \ddot{\theta}_1 \cos \theta_2] \delta(x_2 - x_m), \tag{11}
 \end{aligned}$$

$$v(0, t) = 0, \quad v'(0, t) = 0, \quad v''(l_2, t) = 0, \quad v'''(l_2, t) = 0. \tag{12}$$

Here  $\delta$  is the Dirac delta function, and

$$\begin{aligned}
 I_{T_1} = & I_{h_1} + m_{h_2} (r_{0_1} + l_1)^2 + \frac{1}{3} \rho_1 A_1 (r_{0_1} + l_1)^3 - r_{0_1}^3 + \rho_2 A_2 l_2 (r_{0_1} + l_1)^2 + m (r_{0_1} + l_1)^2 \\
 I_{T_2} = & I_{h_2}, \quad I_T = \frac{1}{3} \rho_2 A_2 (r_{0_2} + l_2)^3 - r_{0_2}^3.
 \end{aligned}$$

The above equations describe the vibration of the flexible link, the rigid body rotations, and the axial displacement of the payload mass relative to the flexible link denoted by  $v, \theta_1, \theta_2$  and  $x_m$ , respectively.

### 3. STABILITY DUE TO PD-TYPE CONTROLLERS

The control torques and force are proposed to be in the form

$$u_{\theta_1} = -K_{P_1}(\theta_1 - \theta_{f_1}) - K_{D_1}\dot{\theta}_1, \tag{13}$$

$$u_{\theta_2} = -K_{P_2}(\theta_2 - \theta_{f_2}) - K_{D_2}\dot{\theta}_2, \tag{14}$$

$$u_{x_m} = -K_{D_3}\dot{x}_m - K_{P_3}(x_m - x_{m_f}), \tag{15}$$

where  $\theta_{f_1}$  and  $\theta_{f_2}$  are the maneuver angles,  $x_{m_f}$  is the desired value of the payload axial displacement. The gains are assumed to be positive. In case that the positions are measured, this control is essentially a proportional plus derivative feedback (PD) controller. If both positions and velocities are measured, then it can be considered as an output feedback. It can be seen that the above control can be easily implemented by using traditional sensors commonly used in robotics. The rotations of the links can be measured by encoders. The relative motion of the payload mass can be measured by a linear variable displacement transducer (LVDT). An indirect measurement may also be feasible through the use of an accelerometer, though this requires the measurement of the link deflection.

One way to prove stability is to select a candidate Lyapunov function and examine its time rate of change. Following the work of Yigit [2], let this function be of the form

$$\begin{aligned} V(t) = & \frac{1}{2} I_{h_1} \dot{\theta}_1^2 + \frac{1}{2} I_{h_2} \dot{\theta}_2^2 + \frac{1}{2} m_{h_2} \dot{\theta}_1^2 (r_{0_1} + l_1)^2 + \frac{1}{2} \rho_1 A_1 \dot{\theta}_1^2 \int_0^{l_1} (r_{0_1} + x_1)^2 dx_1 \\ & + \frac{1}{2} \rho_2 A_2 \int_0^{l_2} \dot{r}_2 \cdot \dot{r}_2 dx_2 + \frac{1}{2} m \dot{r}_m \cdot \dot{r}_m + \frac{1}{2} \int_0^{l_2} EI(v'')^2 dx_2 \\ & + \frac{1}{2} K_{P_1}(\theta_1 - \theta_{f_1})^2 + \frac{1}{2} K_{P_2}(\theta_2 - \theta_{f_2})^2 + \frac{1}{2} K_{P_3}(x_m - x_{m_f})^2. \end{aligned} \tag{16}$$

In order to achieve a global minimum of  $V$  at the desired state the last three terms in the above equation are added. It can be noted that the above function is positive, and is zero at the desired equilibrium. Differentiating  $V$  with respect to time and simplifying the resulting equation yield

$$\dot{V}(t) = \dot{\theta}_1(u_{\theta_1} + K_{P_1}(\theta_1 - \theta_{f_1})) + \dot{\theta}_2(u_{\theta_2} + K_{P_2}(\theta_2 - \theta_{f_2})) + \dot{x}_m(u_{x_m} + K_{P_3}(x_m - x_{m_f})). \tag{17}$$

Substituting equations (13–15) in  $\dot{V}(t)$  gives

$$\dot{V}(t) = -K_{D_1}\dot{\theta}_1^2 - K_{D_2}\dot{\theta}_2^2 - K_{D_3}\dot{x}_m^2, \tag{18}$$

which is negative semi-definite, since  $\dot{\theta}_1, \dot{\theta}_2,$  and  $\dot{x}_m$  can be zero at states other than the desired ones. In order to show the asymptotic stability, LaSalle’s Theorem is employed [16].

Since  $V(t) \equiv 0$  implies that  $\dot{\theta}_1(t) \equiv 0$ ,  $\dot{\theta}_2(t) \equiv 0$  and  $\dot{x}_m \equiv 0$ , and thus,  $\ddot{\theta}_1(t) = 0$ ,  $\ddot{\theta}_2(t) = 0$ , and  $\ddot{x}_m \equiv 0$ . Therefore, equations (8–12) reduce to

$$0 = K_{P_1}(\theta_1 - \theta_{f_1}) + \rho_2 A_2 \int_0^{l_2} [(r_{0_2} + x_2)\ddot{v} + (r_{0_1} + l_1) \cos \theta_2 \ddot{v}] dx_2 + m(r_{0_2} + x_m) \frac{d^2 v_m}{dt^2} + m(r_{0_1} + l_1) \cos \theta_2 \frac{d^2 v_m}{dt^2}, \tag{19}$$

$$0 = K_{P_2}(\theta_2 - \theta_{f_2}) + \rho_2 A_2 \int_0^{l_2} (r_{0_2} + x_2)\ddot{v} dx_2 + m \left[ (r_{0_2} + x_m) \frac{d^2 v_m}{dt^2} \right], \tag{20}$$

$$0 = K_{P_3}(x_m - x_{m_f}) + m v_m' \frac{d^2 v_m}{dt^2}, \tag{21}$$

$$0 = EI v'''' + \rho_2 A_2 \ddot{v} + m \frac{d^2 v_m}{dt^2} \delta(x_2 - x_m), \tag{22}$$

$$v(0, t) = 0, \quad v'(0, t) = 0, \quad v''(l_2, t) = 0, \quad v'''(l_2, t) = 0, \tag{23}$$

where the identity

$$\frac{d^2 v_m}{dt^2} = \ddot{v}_m + 2\dot{x}_m \dot{v}'_m + \dot{x}_m^2 v''_m + \ddot{x}_m v'_m$$

has been used. The solution to equations (22, 23) can be assumed to be in the form

$$v(x, t) = \sum_{i=1}^{\infty} \phi_i(x) q_i(t), \tag{24}$$

where  $\phi_i(x)$  are comparison functions which satisfy the boundary conditions. Note that  $\theta_1 - \theta_{f_1}$ ,  $\theta_2 - \theta_{f_2}$ , and  $x_m - x_{m_f}$  are constants. The substitution of the above equation in equations (19–22) leads to the conclusion that these equations hold only if  $\theta_1 = \theta_{f_1}$ ,  $\theta_2 = \theta_{f_2}$ ,  $x_m = x_{m_f}$  and  $q_i = 0$  for all  $i = 1, 2, \dots, \infty$ , and thus,  $v(x, t) = 0$ . Thus it has been shown that the only solution of the system given by equations (19–23) satisfying  $\dot{V} \equiv 0$  is the null solution (desired states). Therefore, the controlled system is asymptotically stable [16].

At this stage, it should be observed that the proposed controller does not require any state estimation since all quantities used to determine the control forces can be easily measured. Since no discretization of the flexural motion is needed, there is no spillover problem. Furthermore, this control has the stability robustness to parameter uncertainties since the gains are not computed by using the parameters of the system. For all physically reasonable values of the parameters of the system,  $V$  remains to be a valid Lyapunov function.

#### 4. SIMULATION RESULTS

Adopting the Galerkin approach for the discretization of the above equations of motion, let

$$v(x, t) = \sum_{i=1}^N \phi_i(x) q_i(t), \tag{25}$$

where  $N$  is the number of modes that are sufficient to approximate the vibratory motion of the flexible link,  $\phi_i$ 's are comparison functions which satisfy the boundary conditions, and  $q_i$ 's are the modal amplitudes of vibration. Let the assumed modes be those of a non-rotating cantilever beam, i.e.,

$$\phi_i = \cosh \beta_i \frac{x}{l_2} - \cos \beta_i \frac{x}{l_2} - e_i \left( \sinh \beta_i \frac{x}{l_2} - \sin \beta_i \frac{x}{l_2} \right), \tag{26}$$

$$e_i = \frac{\cosh \beta_i + \cos \beta_i}{\sinh \beta_i + \sin \beta_i},$$

where  $\beta_i$ 's are the solutions of

$$\cosh \beta_i \cos \beta_i = -1.$$

Substituting equation (25) into equations (8-11) and writing the resulting equations in the matrix form yield

$$\begin{bmatrix} M_{11} & M_{12} & M_{13} & M_{14} \\ M_{12} & M_{22} & M_{23} & M_{24} \\ M_{13} & M_{23} & M_{33} & M_{34} \\ M_{14}^T & M_{24}^T & M_{34}^T & M_{44}^T \end{bmatrix} \begin{bmatrix} \ddot{\theta}_1 \\ \ddot{\theta}_2 \\ \ddot{x}_m \\ \ddot{q} \end{bmatrix} + \begin{bmatrix} h_{\theta_1} \\ h_{\theta_2} \\ h_{x_m} \\ h_q \end{bmatrix} = \begin{bmatrix} \frac{1}{\rho_2 A_2 l_2} \\ 0 \\ 0 \\ 0 \end{bmatrix} u_{\theta_1} + \begin{bmatrix} 0 \\ \frac{1}{\rho_2 A_2 l_2} \\ 0 \\ 0 \end{bmatrix} u_{\theta_2} + \begin{bmatrix} 0 \\ 0 \\ \frac{1}{\rho_2 A_2 l_2} \\ 0 \end{bmatrix} u_{x_m}, \tag{27}$$

where the superscript T denotes the matrix transpose, and the elements of the mass matrix  $M$  and the non-linear vector  $h$  are given in the appendix.

In all simulations, the following parameter values are used:  $\theta_{f_1} = 1$  rad,  $\theta_{f_2} = 0.5$  rad,  $x_{m_f} = l_2 = 0.762$  m,  $\mu = 0.25$ ,  $l_1 = l_2 = 0.762$  m,  $EI = 0.5473$  N m<sup>2</sup>,  $\rho_1 = \rho_2 = 2710$  kg/m<sup>3</sup>,  $A_1 = 1.613 \times 10^{-4}$  m<sup>2</sup>,  $A_2 = 3.226 \times 10^{-5}$  m<sup>2</sup>,  $r_{0_1} = r_{0_2} = 0.09525$  m,  $I_{h_1} = I_{h_2} = 0.0017628$  kg m<sup>2</sup>,  $m_{h_2} = 0.3886$  kg,  $K_{p_1} = 7.3365$  N m/rad,  $K_{p_2} = 0.3215$  N m/rad,  $K_{D_1} = 2.5938$  N m s/rad,  $K_{D_2} = 0.1137$  N m s/rad,  $K_{p_3} = 2.3982$  N/m,  $K_{D_3} = 1.2491$  N s/m. The number of modes to be taken depends on the excitations (i.e., input torques and forces). It has been verified through numerical simulations that a three-mode approximation is sufficient to model the vibratory motion of the flexible link for the maneuvers considered. The frequencies of the first three modes are 15.15, 94.94 and 265.87 rad/s respectively. The feedback gains are selected on the basis that the damping ratio associated with the rigid-body motion is approximately 0.707.

First, let the payload mass be fixed at the tip of the flexible link, and the control action for the axial motion is turned off ( $K_{p_3} = 0$ ,  $K_{D_3} = 0$ ). Figures 2(a-d) display the angular displacements  $\theta_1$  and  $\theta_2$ , the tip deflection  $v(l_2, t)$ , the payload deflection  $v_m(x_m, t)$ , and the torque inputs  $u_{\theta_1}$  and  $u_{\theta_2}$ . Note that since the payload mass is kept at the tip,  $v(l_2, t) = v_m(x_m, t)$  at all times. As expected, the controller is able to control the motion and suppresses the vibrations induced by the maneuver. However, there is a large elastic deflection in the beginning of the maneuver. Thus, the payload is subjected to large accelerations during this time. Clearly, by reducing the controller gains, this large acceleration can be avoided at the expense of slowing down the system response.

Next, let the payload mass be initially at  $x_2 = 0$ , and is allowed to move under the control action. The resulting performance is shown in Figures 3(a-f) from which the following observations can be made.



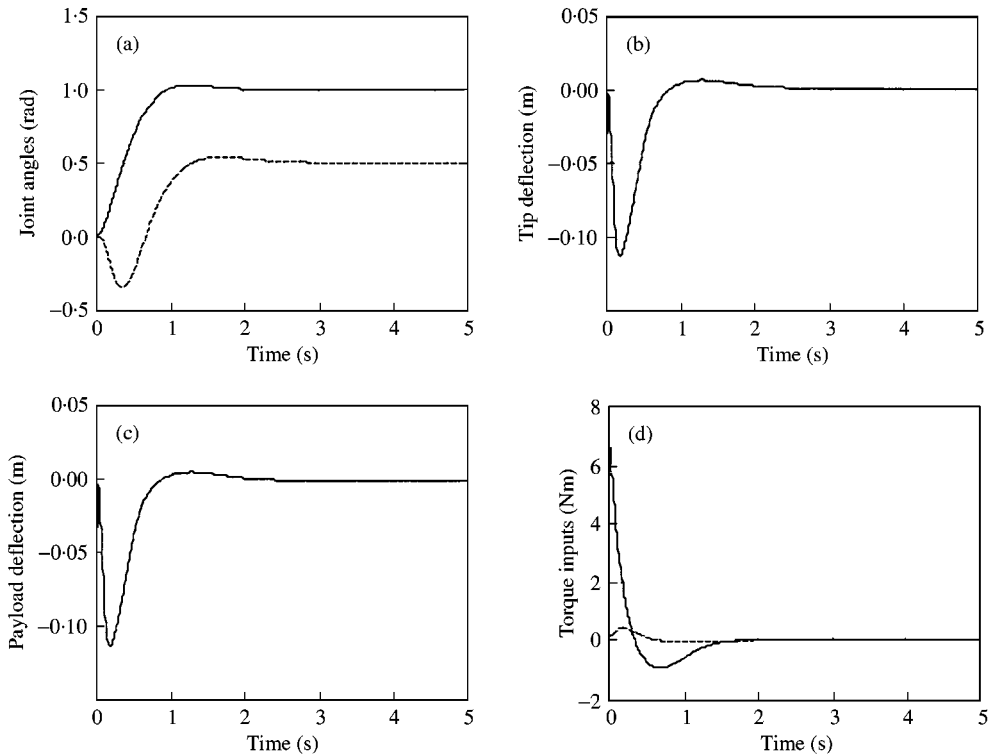


Figure 2. Performance of the manipulator with no relative motion of the payload mass; —, shoulder joint; - - -, elbow joint.

1. The axial motion of the payload mass alters the dynamics of the rigid body motions, causing more oscillatory angular displacements. This can be justified by the existence of the Coriolis accelerations which include the terms  $m\dot{\theta}\dot{x}_m$  and  $m\dot{\theta}\dot{v}_m$  (see equations (8, 9)).
2. It introduces additional damping to the link vibratory motion through the acceleration term  $2\mu\dot{x}_m\dot{v}_m$  in equation (11).
3. The vibratory motion of the payload mass is reduced considerably, due to the fact that it starts in a region near the rigid base which experiences less vibrational amplitudes. This is an advantage in the sense that the axial motion offers a solution to slewing flexible structures, such as maneuverable space structures, which carry humans or sensitive objects.
4. The maximum values of the torque inputs are not affected significantly by the axial motion of the payload mass. This constitutes an advantage in the sense that the axial motion of the payload mass introduces more structural damping while maintaining the same maximum torque input requirement.

Developed above are driving torques and regulating force for the motion control of the manipulator. Although, the desired final state can be achieved, the trajectories undertaken by the rigid-body rotations and the payload axial motion during maneuver cannot be fully controlled. This suggests that the torques and force be modified for tracking reference trajectories.

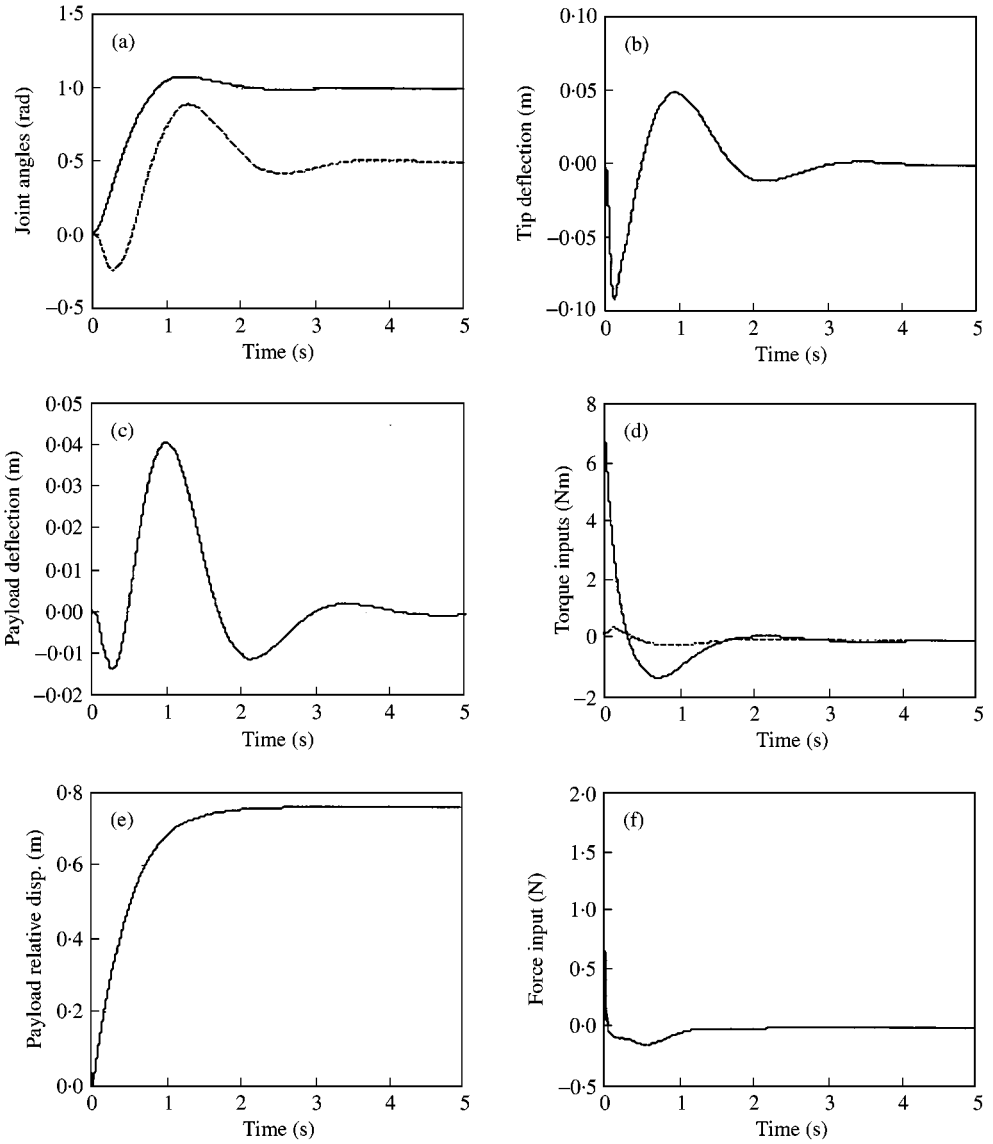


Figure 3. Performance of the manipulator with relative motion of the payload mass; key as in Figure 2.

### 5. STABILITY FOR TRACKING REFERENCE TRAJECTORIES

Suppose it is preferred that the rigid-body rotations and the payload axial motion track a prespecified set of reference trajectories denoted by  $\theta_{1r}$ ,  $\theta_{2r}$ , and  $x_{mr}$ . In addition, the vibratory motion can also be assigned a zero-reference trajectory. In this case, the torques applied at the rigid bases are modified as

$$\begin{aligned}
 u_{\theta_1} &= u_{\theta_{1r}} - K_{P_1}(\theta_1 - \theta_{1r}) - K_{D_1}(\dot{\theta}_1 - \dot{\theta}_{1r}), \\
 u_{\theta_2} &= u_{\theta_{2r}} - K_{P_2}(\theta_2 - \theta_{2r}) - K_{D_2}(\dot{\theta}_2 - \dot{\theta}_{2r}), \\
 u_{x_m} &= u_{x_{mr}} - K_{P_3}(x_m - x_{mr}) - K_{D_3}(\dot{x}_m - \dot{x}_{mr}),
 \end{aligned}
 \tag{28}$$

where  $u_{\theta_{1r}}$ ,  $u_{\theta_{2r}}$  and  $u_{x_{mr}}$  are the feedforward control inputs. The reference trajectories  $\theta_{1r}$ ,  $\theta_{2r}$  and  $x_{mr}$  are determined using inverse kinematics or inverse dynamics algorithms [17, 18]. For instance, these trajectories are determined from specifying a reference path of the payload mass. The resulting reference trajectories can be used to determine the required feedforward control inputs as

$$\begin{aligned} u_{\theta_{1r}} = & I_{T_1} \ddot{\theta}_{1r} + I_T \ddot{\theta}_r \\ & + \frac{1}{2} \rho_2 A_2 (r_{0_1} + l_1) [(r_{0_2} + l_2)^2 - r_{0_2}^2] [2(\ddot{\theta}_{1r} + \ddot{\theta}_{2r}) \cos \theta_{2r} - (\dot{\theta}_{2r}^2 + 2\dot{\theta}_{1r} \dot{\theta}_{2r}) \sin \theta_{2r}] \\ & + m [(r_{0_2} + x_{mr}) ((r_{0_2} + x_{mr}) \ddot{\theta}_r + 2\dot{x}_{mr} \dot{\theta}_r)] + m (r_{0_1} + l_1) \cos \theta_{2r} [(r_{0_2} + x_{mr}) (2\ddot{\theta}_{1r} \\ & + \ddot{\theta}_{2r}) + 2\dot{\theta}_r \dot{x}_{mr}] - m (r_{0_1} + l_1) \sin \theta_{2r} [(r_{0_2} + x_{mr}) (2\dot{\theta}_{1r} \dot{\theta}_{2r} + \dot{\theta}_{2r}^2) - \ddot{x}_{mr}], \end{aligned} \quad (29)$$

$$\begin{aligned} u_{\theta_{2r}} = & I_{T_2} \ddot{\theta}_{2r} + I_T \ddot{\theta}_r + \frac{1}{2} \rho_2 A_2 [(r_{0_2} + l_2)^2 - r_{0_2}^2] (r_{0_1} + l_1) (\ddot{\theta}_{1r} \cos \theta_{2r} + \dot{\theta}_{1r}^2 \sin \theta_{2r}) \\ & + m [(r_{0_2} + x_{mr}) ((r_{0_2} + x_{mr}) \ddot{\theta}_r + 2\dot{x}_{mr} \dot{\theta}_r)] \\ & + m (r_{0_1} + l_1) [(r_{0_2} + x_{mr}) (\ddot{\theta}_{1r} \cos \theta_{2r} + \dot{\theta}_{1r}^2 \sin \theta_{2r})], \end{aligned} \quad (30)$$

$$u_{x_{mr}} = m [\ddot{x}_{mr} - (r_{0_2} + x_{mr}) \dot{\theta}_r^2 + (r_{0_1} + l_1) (\ddot{\theta}_{1r} \sin \theta_{2r} - \dot{\theta}_{1r}^2 \cos \theta_{2r})]. \quad (31)$$

In order to verify the stability of the manipulator with reference trajectories, one may use the Lyapunov stability method. A candidate Lyapunov function similar to the one used earlier can be constructed. However, it was difficult to show that the time rate of change of  $V$  is negative semi-definite. The complexity occurred because of the dependence of the reference trajectory on time. Stability can also be proven if the equations of motion are linearized about the desired state [2] by Lyapunov's indirect method. However, the issue of asymptotic stability for the case of tracking an arbitrary trajectory is not pursued further in the current work. It should be noted that the modified control law given in equation (28) is now a model-based controller and suffers from the shortcomings mentioned in the introduction. Thus, stability robustness to parameter uncertainties must be accounted for in the design process through the feedback gains.

Several simulations were performed to examine the performance of the system for reference trajectories. For instance, let

$$\begin{aligned} \theta_{1r} = & \begin{cases} 6 \left( \frac{t}{t_{f_1}} \right)^5 - 15 \left( \frac{t}{t_{f_1}} \right)^4 + 10 \left( \frac{t}{t_{f_1}} \right)^3, & t < t_{f_1} \\ 1, & t \geq t_{f_1} \end{cases} \\ \theta_{2r} = & \begin{cases} \frac{1}{2} \left( 6 \left( \frac{t}{t_{f_2}} \right)^5 - 15 \left( \frac{t}{t_{f_2}} \right)^4 + 10 \left( \frac{t}{t_{f_2}} \right)^3 \right), & t < t_{f_2} \\ \frac{1}{2}, & t \geq t_{f_2} \end{cases} \\ x_{mr} = & \begin{cases} l_2 \left( 6 \left( \frac{t}{t_{f_3}} \right)^5 - 15 \left( \frac{t}{t_{f_3}} \right)^4 + 10 \left( \frac{t}{t_{f_3}} \right)^3 \right), & t < t_{f_3} \\ l_2, & t \geq t_{f_3} \end{cases}. \end{aligned}$$

Figures 4(a-f) show the resulting performance for  $t_{f_1} = t_{f_2} = 2$  s,  $t_{f_3} = 3.5$  s,  $K_{P_3} = 3.2643$ , and  $K_{D_3} = 0.2332$ . As can be seen, the tracking performance is very good with respect to

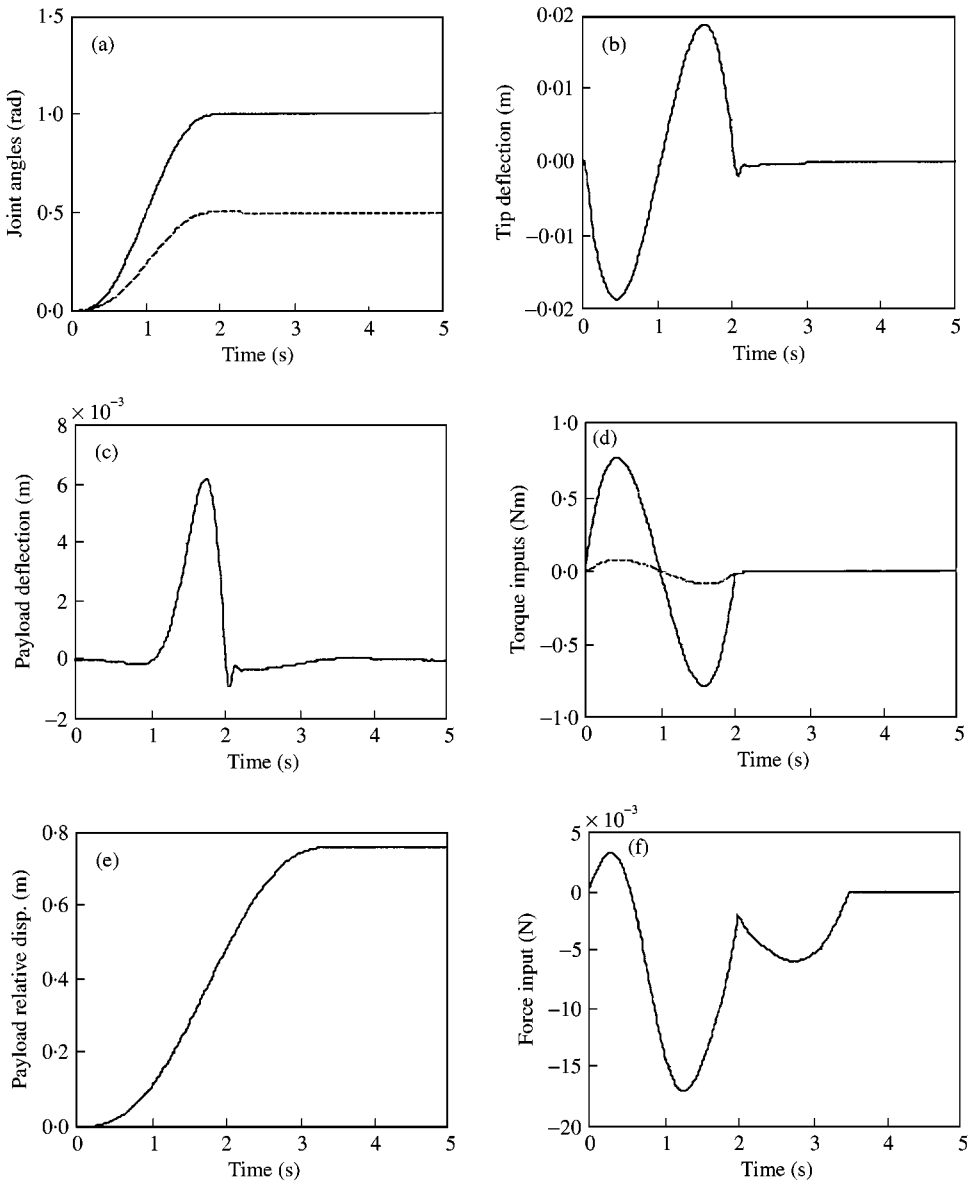


Figure 4. Performance of the manipulator with reference trajectories; key as in Figure 2.

link rotations. Tip deflection is reduced significantly due to the smooth nature of reference trajectories, and overall maneuver time is very close to that of the previous case. More importantly, the control torque and force magnitudes are an order of magnitude lower than the set point controller presented in section 4.

### 6. SUMMARY AND CONCLUSIONS

A mathematical model of a two-link rigid-flexible manipulator carrying a moving payload mass was derived. Two joint motor torques were applied at the rigid hubs for the

motion control of both links, in addition to a force actuator which controls the payload relative motion. With the aid of a candidate Lyapunov function, it was shown that the use of the proposed PD-type controller stabilizes the system maneuvering dynamics in which the payload is allowed to move relative to the flexible link in the axial direction. These torques yield a convergence of residual vibration to zero, an attainment of the rigid-body rotations to their prespecified desired angles of maneuver, and an axial guidance of the payload mass to the desired location along the flexible link. It was shown that allowing the relative motion of the payload mass in a prescribed manner leads to a considerable reduction of its residual vibration as compared with the case when it is fixed to the link tip during the time of maneuver. Stability was also verified through numerical simulation in case the rigid-body motions track prespecified reference trajectories. It is believed that the results of this study can be extended to flexible multi-link manipulators, and thus, can be of great importance for slewing space structures where the transported object is sensitive to vibrations.

Future work should focus on implementation issues and experimental realization of the proposed manipulator. Clearly, there will be some design challenges for realizing the relative payload motion on a flexible link. Depending on the drive system used, there will be limitations on the allowable deflections of the flexible link. It should be noted, however, that with the payload motion, the flexible link is shown to experience much smaller deflections. Therefore, this problem may not be as severe as it seems. The inevitable friction between the payload and the link, which is neglected in the current work, should be considered. It may be necessary to compensate this non-linearity through feedback. The effects of sensor noise and actuator saturation should also be examined.

#### REFERENCES

1. N. K. HECHT and J. L. JUNKINS 1992 *Journal of Guidance, Control, and Dynamics* **15**, 477–481. Near-minimum-time control of a flexible manipulator.
2. A. S. YIGIT 1994 *Journal of Dynamic Systems, Measurement and Control* **116**, 208–215. On the stability of PD control for a two-link rigid-flexible manipulator.
3. W. J. BOOK, O. MAIZZA-NETA and D. E. WHITNEY 1975 *Journal of Dynamic Systems, Measurement and Control* **97**, 424–431. Feedback control of two beam, two joint systems with distributed flexibility.
4. R. H. CANNON, Jr. and E. SCHMITZ 1984 *The International Journal of Robotics Research* **3**, 62–75. Initial experiments on the end-point control of a flexible one-link robot.
5. A. S. MORRIS and A. MADANI 1998 *Robotica* **16**, 97–108. Quadratic optimal control of a two-link flexible-link manipulator.
6. H. ASADA and J. J. E. SLOTINE 1986, *Robot Analysis and Control*, New York: John Wiley and Sons, Inc.
7. M. KARKOUB, K. TAMMA and G. BALAS 1999 *Journal of Vibration and Control* **5**, 559–576. Robust control of two-link flexible manipulators using the mu-synthesis technique.
8. S.-B. CHOI, C.-C. CHEONG and H.-C. SHIN 1995 *Journal of Sound and Vibration* **179**, 737–748. Sliding mode control of vibration in a single-link flexible arm with parameter variations.
9. M. J. BALAS 1978 *IEEE Transactions on Automatic Control* **AC-23**, 673–679. Feedback control of flexible systems.
10. K. YUAN 1997 *Journal of Sound and Vibration* **204**, 795–806. Control of slew maneuver of a flexible beam mounted non-radially on a rigid hub: a geometrically exact modeling approach.
11. K. YUAN and C. M. TSAI 1998 *Proceedings of the Sixth IASTED International Conference on Robotics and Manufacturing, Baff, Canada, July 26–29*, 133–139. Stability of PD control for a two-link rigid-flexible manipulator: a geometrically exact modeling approach.
12. S. S. GEE, T. H. LEE and G. ZHU 1996 *Mechatronics* **6**, 779–798. Energy-based robust controller design for multi-link flexible robots.
13. E. SCHMITZ and M. Ramey 1990, *International Conference on Dynamics of Flexible Structures in Space, Cranfield, England, U.K., May 15–18*. Experiments in active control for large space manipulators.

14. H. G. LEE, S. ARIMOTO and F. MIYAZAKI 1988 *Proceedings of the 27th Conference of Decision and Control, Institute of Electrical and Electronic Engineers, New York*, 75–80. Liapunov stability analysis for DPS control of flexible multi-link manipulators.
15. S. CHOURA 1997 *Proceedings of the Institution of Mechanical Engineers Part I-Journal of Systems and Control* Vol. 211, 25–34. Reduction of residual vibrations in a rotating flexible-beam with a moving payload mass.
16. VIDYASAGAR, M., 1978, *Nonlinear Systems Analysis*, Englewood, Cliffs, NJ: Prentice Hall.
17. H. ASADA, Z. D. MA and H. TOKUMARU 1990 *Journal of Dynamic Systems, Measurement, and Control* **112**, 177–185. Inverse dynamics of flexible robot arms: modeling and computation of trajectory control.
18. E. BAYO, P. PAPADOPOULOS and J. STUBBE 1989 *The International Journal of Robotics Research* **8**, 49–62. Inverse dynamics and kinematics of multi-link elastic robots: an iterative frequency domain approach.

APPENDIX A

$$M_{11} = \frac{I_{T_1} + I_T}{\rho_2 A_2 l_2} + \sum_{i=1}^N q_i^2 - 2(r_{0_1} + l_1) \sin \theta_2 \sum_{i=1}^N b_i q_i + 2 \frac{(r_{0_2} + l_2)^2 - r_{0_2}^2}{2l_2} (r_{0_1} + l_1) \cos \theta_2$$

$$+ \mu(r_{0_2} + x_m)^2 + \mu v_m^2 + 2\mu(r_{0_1} + l_1)(r_{0_2} + x_m) \cos \theta_2 - 2\mu(r_{0_1} + l_1)v_m \sin \theta_2,$$

$$M_{12} = \frac{I_T}{\rho_2 A_2 l_2} + \sum_{i=1}^N q_i^2 - (r_{0_1} + l_1) \sin \theta_2 \sum_{i=1}^N b_i q_i + \frac{(r_{0_2} + l_2)^2 - r_{0_2}^2}{2l_2} (r_{0_1} + l_1) \cos \theta_2$$

$$+ \mu(r_{0_2} + x_m)^2 + \mu v_m^2 + \mu(r_{0_1} + l_1)(r_{0_2} + x_m) \cos \theta_2 - \mu(r_{0_1} + l_1)v_m \sin \theta_2,$$

$$M_{13} = \mu v'_m (r_{0_2} + x_m)^2 - \mu v_m + \mu(r_{0_1} + l_1)v'_m \cos \theta_2 + \mu(r_{0_1} + l_1) \sin \theta_2,$$

$$(M_{14})_i = a_i + (r_{0_1} + l_1)b_i \cos \theta_2 + \mu(r_{0_2} + x_m)\phi_i(x_m)$$

$$+ \mu(r_{0_1} + l_1) \cos \theta_2 \phi_i(x_m), \quad i = 1, 2, \dots, N,$$

$$M_{22} = \frac{I_{T_2} + I_T}{\rho_2 A_2 l_2} + \sum_{i=1}^N q_i^2 + \mu(r_{0_2} + x_m)^2 + \mu v_m^2,$$

$$M_{23} = \mu(r_{0_2} + x_m)v'_m - \mu v_m,$$

$$(M_{24})_i = a_i + \mu(r_{0_2} + x_m)\phi_i(x_m), \quad i = 1, 2, \dots, N,$$

$$M_{33} = \mu(1 + (v'_m)^2),$$

$$(M_{34})_i = \mu v'_m \phi_i(x_m), \quad i = 1, 2, \dots, N,$$

$$(M_{44})_{ij} = \begin{cases} 1 + \mu(\phi_i(x_m))^2 & \text{if } i = j \\ \mu\phi_i(x_m)\phi_j(x_m) & \text{if } i \neq j \end{cases} \quad i, j = 1, 2, \dots, N,$$

$$h_{\theta_1} = 2\dot{\theta} \sum_{i=1}^N q_i \dot{q}_i - 2\dot{\theta}(r_{0_1} + l_1) \sin \theta_2 \sum_{i=1}^N b_i \dot{q}_i - \dot{\theta}_2(2\dot{\theta}_1 + \dot{\theta}_2)(r_{0_1} + l_1) \cos \theta_2 \sum_{i=1}^N b_i q_i$$

$$- \frac{(r_{0_2} + l_2)^2 - r_{0_2}^2}{2l_2} (r_{0_1} + l_1) \dot{\theta}_2(2\dot{\theta}_1 + \dot{\theta}_2) \sin \theta_2$$

$$\begin{aligned}
& + \mu[(r_{0_2} + x_m)(2\dot{x}_m\dot{\theta} + 2\dot{x}_m\dot{v}'_m + \dot{x}_m^2 v''_m) + 2v_m\dot{v}_m\dot{\theta} + 2v_m v'_m \dot{x}_m \dot{\theta}] \\
& + \mu(r_{0_1} + l_1) \cos \theta_2 [2\dot{x}_m\dot{\theta} - (\dot{\theta}_2^2 + 2\dot{\theta}_1\dot{\theta}_2)v_m + 2\dot{v}'_m \dot{x}_m + \dot{x}_m^2 v''_m] \\
& - \mu(r_{0_1} + l_1) \sin \theta_2 [(r_{0_2} + x_m)(2\dot{\theta}_1\dot{\theta}_2 + \dot{\theta}_2^2) + 2\dot{\theta}\dot{v}_m + 2\dot{\theta}\dot{x}_m v'_m], \\
h_{\theta_2} = & 2\dot{\theta} \sum_{i=1}^N q_i \dot{q}_i + \dot{\theta}_1^2 (r_{0_1} + l_1) \cos \theta_2 \sum_{i=1}^N b_i q_i + \frac{(r_{0_2} + l_2)^2 - r_{0_2}^2}{2l_2} (r_{0_1} + l_1) \dot{\theta}_1^2 \sin \theta_2 \\
& + \mu[(r_{0_2} + x_m)(2\dot{x}_m\dot{\theta} + 2\dot{x}_m\dot{v}'_m + \dot{x}_m^2 v''_m) + 2v_m\dot{v}_m\dot{\theta} + 2v_m v'_m \dot{x}_m \dot{\theta}] \\
& + \mu(r_{0_1} + l_1) \dot{\theta}_1^2 [(r_{0_2} + x_m) \sin \theta_2 + v_m \cos \theta_2], \\
h_{x_m} = & \mu[2\dot{x}_m v'_m \dot{v}'_m + \dot{x}_m^2 v'_m v''_m - 2\dot{\theta}\dot{v}_m - (r_{0_2} + x_m)\dot{\theta}^2 \\
& - v_m v'_m \dot{\theta}^2 - (r_{0_1} + l_1) \dot{\theta}_1^2 \cos \theta_2 + (r_{0_1} + l_1) \dot{\theta}_1^2 v'_m \sin \theta_2], \\
(h_q)_i = & (\omega_i^2 - \dot{\theta}^2) q_i + \dot{\theta}_1^2 (r_{0_1} + l_1) b_i \sin \theta_2 \\
& + \mu[-v_m \dot{\theta}^2 + 2\dot{x}_m \dot{\theta} + 2\dot{v}'_m \dot{x}_m + \dot{x}_m^2 v''_m + (r_{0_1} + l_1) \dot{\theta}_1^2 \sin \theta_2] \phi_i(x_m),
\end{aligned}$$

where

$$\mu = \frac{m}{\rho_2 A_2 l_2}, \quad \omega_i = \beta_i^2 \left( \frac{EI}{\rho_2 A_2 l_2^4} \right)^{1/2}, \quad a_i = \frac{1}{l_2} \int_0^{l_2} (r_{0_2} + x_2) \phi_i(x_2) dx_2, \quad b_i = \frac{1}{l_2} \int_0^{l_2} \phi_i(x_2) dx_2.$$